The distorted close-packed crystal structure of methane A

The distorted close-packed crystal structure of methane A

H. E. Maynard-Casely,[a] C. L. Bull, M. Guthrie,[b] I. Loa, M. I. McMahon, E. Gregoryanz, R. J. Nelmes, and J. S. Loveday
SUPA, School of Physics and Astronomy, Centre for Science at Extreme Conditions, The University of Edinburgh, Edinburgh EH9 3JZ, United Kingdom

(Received 25 February 2010; accepted 31 May 2010; published online 9 August 2010)

We have determined the full crystal structure of the high-pressure phase methane A. X-ray single-crystal diffraction data were used to determine the carbon-atom arrangement, and neutron powder diffraction data from a deuterated sample allowed the deuterium atoms to be located. It was then possible to refine all the hydrogen positions from the single-crystal x-ray data. The structure has 21 molecules in a rhombohedral unit cell, and is quite strongly distorted from the cubic close-packed structure of methane I, although some structural similarities remain. Full knowledge of this structure is important for modeling of methane at higher pressures, including in relation to the mineralogy of the outer solar system. We discuss interesting structural parallels with the carbon tetrahalides. © *2010 American Institute of Physics*. [doi:10.1063/1.3455889]

I. INTRODUCTION

Methane is one of the major constituents of the gas-giant planets Uranus and Neptune in the outer solar system, and accreted into these planets during their formation from the solar nebula. They are similar in size, mass, and composition, and have an interior structure described in terms of three distinct regions.[1] The outermost layer contains a mixture of primarily hydrogen, helium, water, methane, and ammonia in that order of abundance, and covers the pressure range up to 10 GPa and temperatures of 70–2000 K. In the middle layer, pressure and temperature increase from 10 GPa and 2000 K to approximately 800 GPa and 8000 K with increasing depth. This second layer accounts for the majority of the planets' volume and mass, and it is composed of molecular ices (water, methane, and ammonia), and possibly a silicate component. The third layer is a dense silicate and metal core.[1] Under the conditions of the middle layer, methane, ammonia, and water will be dense fluids with, in some cases, a significant degree of ionization, and it is believed that the complex magnetic fields of Uranus and Neptune are the result of convection in this middle ice layer.[2] Because the conditions of the middle ice layer are difficult or impossible to access experimentally, modeling of its behavior currently relies on computational studies of the properties of the constituent materials. Such studies benefit from experimental data on the solid phases at high pressure as benchmarks for testing computational predictions. In the case of water and ammonia, both experimental and computational studies at high pressure and temperature have been extensively pursued.[3–5] By contrast, the understanding of methane under these conditions is much less well established, with not even the density definitively known above 5 GPa.

Methane is the only member of the group of simple molecular ices (water, methane, ammonia, and hydrogen fluoride) that does not form hydrogen bonds, and its molecular interactions are dominated by the interplay between van der Waals attractions and steric repulsions. The density dependence of the structure and properties of methane provides insight into these interactions without the complications of competing hydrogen bonds, and thus insight also into this type of molecular state. However, in view of the considerable interest and significance of the high-pressure behavior of methane, surprisingly little is yet known about its high-pressure phases and their structures.

Figure 1 shows the current state of knowledge of the P-T

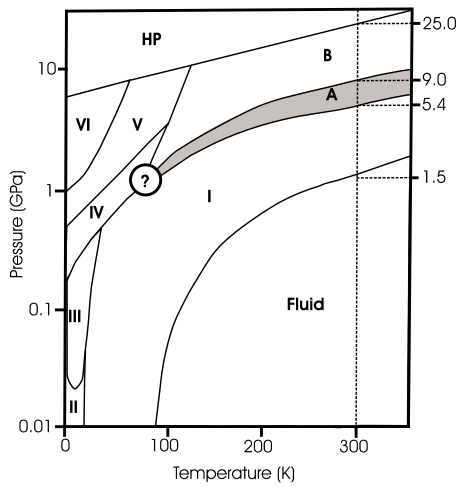

FIG. 1. The current phase diagram of methane as mapped out and drawn by Bini and Pratesi (Ref. 6) and including the addition of phase II by Umemoto *et al.* (Ref. 7). Phases are labeled as discussed in the text. The question mark indicates an area where the boundaries have not yet been determined, and the stability region of methane A is shaded. Transition pressures at room temperature are given in gigapascal on the right-hand vertical axis. As discussed in the text, the transition from methane A to B has been observed as low as 9 GPa (the pressure shown) and as high as 14 GPa, and the reverse transition from B to A has been observed to occur down to 7 GPa.

[a]Present address: School of Chemistry and Centre for Science at Extreme Conditions, The University of Edinburgh, Edinburgh EH9 3JZ, United Kingdom. Electronic mail: h.e.maynard-casely@ed.ac.uk.
[b]Present address: EFree, Carnegie Institution of Washington, Washington DC 20015, USA.

phase diagram. Of the nine solid phases distinguished, crystal structures have been determined only for methane I, II, and III.[8,9] The phase labeled A was discovered by Hazen *et al.*[10] who compressed a single-crystal sample of methane I to just above 5 GPa at room temperature, where the sample transformed to a powder, suggesting that the transition was reconstructive and first-order in nature. Later, Hebert *et al.*[11] studied this transition in more detail using Raman scattering measurements, and confirmed a first-order transformation from methane I at 300 K and 5.4 GPa. Hebert *et al.* labeled the high-pressure form as methane IV because they took it to be the same phase as that previously identified as forming from methane III at 4.2 K and 0.49 GPa (Ref. 12) (see Fig. 1). But the room temperature phase was later distinguished and labeled methane A by Bini *et al.*[13] who reasoned that there was not sufficient evidence to identify it as methane IV. The P-T conditions and nature of the transition between methane IV and A remained unknown.

Under compression at room temperature, methane A transforms to a further modification, originally labeled methane VII,[11] but later renamed as methane B by Bini *et al.*[13] The methane A to B transition has been termed "sluggish." It has been observed to occur at 9 GPa with increasing pressure (Fig. 1) but sometimes not until 14 GPa, and the B to A transition on decreasing pressure can occur down to 7 GPa.[6,11] In a subsequent paper, Bini and Pratesi[6] probed methane's structural behavior more completely by conducting spectroscopic measurements from 50 to 300 K and up to 30 GPa. The phase diagram shown in Fig. 1 is largely based on these studies and includes the low-temperature phases V and VI as labeled. However, this work did not clarify the relationship between the low-temperature phases IV, V, and VI and phases A and B at higher temperatures. Figure 1 also shows a further phase of methane found to form from methane B at 25 GPa on upstroke at room temperature, and Bini and Pratesi[6] proposed it to be hexagonal and labeled it HP. Phases A and B were then taken to be intermediate structures between the rotationally disordered cubic close-packed (CCP) methane I and the proposed ordered hexagonal close-packed HP structure.[6]

All previous structural studies of methane A have been based on spectroscopic and powder diffraction experiments. Both methane IV and A were first interpreted as having tetragonal structures, but later powder diffraction data[14] showed methane A to have a rhombohedral unit cell [$a=8.643(1)$ Å and $\alpha=89.40(2)°$ at 7.0 GPa and room temperature]. On the basis of density in relation to methane I, and symmetry considerations, Nakahata *et al.*[14] assigned 21 molecules to the unit cell. They also pointed out the similarities to high-pressure phases of CCl_4 (phase Ib) and CF_4 (phase I), which have rhombohedral unit cells with $\alpha \approx 89.5°$, believed to contain 21 molecules (see Sec. IV), thus suggesting a common structural progression for methane and the carbon tetrahalides.

Our own recent neutron diffraction measurements on deuterated methane have questioned the low-temperature part of the phase diagram (Fig. 1) and the existence of distinct phases IV, V, and VI.[15] Powder diffraction profiles collected from CD_4 between 1 and 5 GPa from 20 to 100 K (within the stability fields proposed by Bini and Pratesi[6] for methane IV, V, and VI) found only rhombohedral methane A, suggesting that phases IV, V, and VI are not structurally distinct from methane A. We note that this would require some revision of the phase diagram below 100 K.

A detailed structural study of methane A under *in situ* conditions is challenging. The apparent large number of molecules in the unit cell suggests that single-crystal methods may be needed to solve the structure, but a previous attempt to compress a single crystal of methane I into methane A produced only a polycrystalline aggregate, as noted above.[10] The alternative of growing a single crystal within the P-T field of the phase is difficult for a phase not in contact with the melting line. And x-ray data collected under high-pressure conditions, even from a single crystal, are not likely to locate the numerous hydrogen atoms in the structure. This requires neutron diffraction techniques, but single crystals of sufficient size cannot yet be grown *in situ* for work above 5 GPa.[16] Although neutron powder-diffraction techniques can be used, the limited sample volume in a neutron-diffraction pressure cell[17] makes it difficult to collect data of sufficient quality for solution of a complex structure. However, we first succeeded in obtaining good single crystals for x-ray data collection (by crystallizing at ~400 K) from which the carbon (C) atom positions were determined, and were then able to locate the hydrogen (H) atoms [in fact, deuterium (D) atoms as CD_4] from neutron powder diffraction data on the assumption that the molecules were regular tetrahedra. And these H(D) positions were used for a final full refinement of the structure from the x-ray single-crystal data.

II. EXPERIMENTAL

As said, we have taken a combined approach to this investigation using x-ray single-crystal diffraction data and neutron powder diffraction data. For the x-ray single-crystal studies, research grade methane (CH_4) from Sigma Aldrich (with purity 99.995%) was cryogenically loaded into a Merrill–Bassett (MB) diamond-anvil cell,[18] and contained by a rhenium gasket. We used MB cells equipped with Boehler-Almax seats and diamond anvils[19] to optimize the angular access. This method of mounting the diamond anvils also avoids the data containing diffraction lines from any supporting seat under the anvils. Pressure was measured from the fluorescence shift of a small ruby chip (10–15 μm) included in the sample volume.[20,21]

After cryogenic loading, the MB cells were warmed to room temperature and the sample pressure was increased to ~10 GPa for the single-crystal growth. The MB cells were then fitted with an external heater and placed into an apparatus that monitored the temperature of the cell while the sample was kept under visual observation. Each cell was heated to ~400 K at ~9 GPa to take the sample through the transition from methane A to methane I at ~370 K (Fig. 1). Crystals were then grown by cooling back through the methane I to A transition, as illustrated in Fig. 2, by using a thermal sink to create a seed crystal and carefully allowing this to grow with cooling.

Single-crystal x-ray diffraction data were collected on

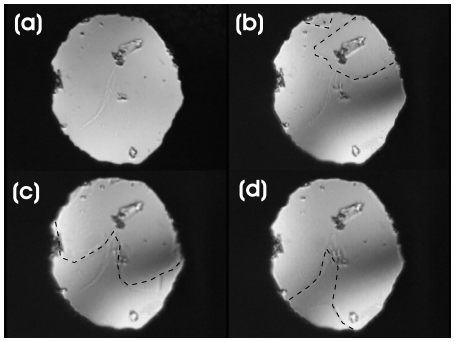

FIG. 2. A crystal of methane A growing at a solid-solid transition between methane I and methane A at 9.3(4) GPa, in a gasket hole that is 100 μm in diameter. The crystal boundaries are clear in original images but difficult to discern and so are indicated with dashed lines here. The small, separate crystallites evident in all the images are pieces of ruby. (a) is at the highest temperature of 410 K after the seed crystal of methane A was created by cooling the cell on one side; (b) is at 400 K, as the seed crystal starts to grow from the top right on cooling; the growth process then continues with further cooling in (c) and (d), and eventually (not shown) the growth progresses to fill the whole sample volume.

station ID09a at the European Synchrotron Radiation Facility (ESRF), Grenoble, and station 9.5HPT, Synchrotron Radiation Source (SRS), Daresbury Laboratory using the procedures outlined in Ref. 22. The first data set was collected from a crystal at 13.6(2) GPa (toward the high end of the methane A stability range), on station ID09a at ESRF, using a wavelength of 0.41 Å and a mar345 image-plate detector placed 200 mm from the sample. These data were collected in sequential 0.33° steps over a total scan range of ±30° around the vertical rotation axis, with an exposure time of 5 s at each step. This yielded 720 measurable reflections to a resolution of 0.8 Å, and gave an $R_{\text{merge}}(F^2)$ of 0.06 (in the $\bar{3}$ Laue class—see below). The data were corrected for absorption by the diamond anvils, for variations in the detector efficiency with scattering angle, and for variations in the sample scattering with the diamond-anvil cell orientation.

A second data set, from a separately grown crystal at 9.1(2) GPa, was collected on station 9.5HPT at SRS, using an x-ray wavelength of 0.44 Å with a sample to detector distance of 340 mm. Some typical data from this data set are shown in Fig. 3. The diffraction images were collected in 0.5° steps over ±30°, at 15 s per frame. This resulted in 679 measured reflections to a resolution of 0.9 Å, and gave an $R_{\text{merge}}(F^2)$ of 0.05 (in the $\bar{3}$ Laue class—see below), after corrections as for the first data set.

Neutron powder data were collected on the HiPr/PEARL instrument at the ISIS Facility, Rutherford Appleton Laboratory, U.K., using a Paris-Edinburgh press[17] fitted with sintered diamond anvils and loaded with pure 99% deuterated CD_4 (Ref. 23) (supplied by Sigma-Aldrich). The effect of deuteration on methane at high pressure and room temperature is unknown, but is expected to be small and not to influence the crystal structures. The CD_4 sample was loaded cryogenically into an encapsulated gasket between the anvils[24] using methods previously described.[25] So as to maximize signal-to-background from the sample, no pressure calibrant was used.

After loading, the sample was returned to room temperature before being taken up in pressure. As there was no pressure marker in the sample, the load (force) applied to the pressure cell was increased until approximately the required pressure was reached—as judged by the normal relationship between load and sample pressure—and then adjusting until the known diffraction pattern for methane A was obtained. The final sample pressure was estimated as 11.4±0.2 GPa from the measured lattice parameters and the CH_4 equation of state determined by Nakahata *et al.*[14] For data collection, the sample was cooled to 110 K with liquid nitrogen to reduce atomic thermal motion in the sample, and thereby improve signal-to-background. The data were corrected for cell attenuation[26] and the program GSAS (Ref. 27) was used for crystal structure refinement.

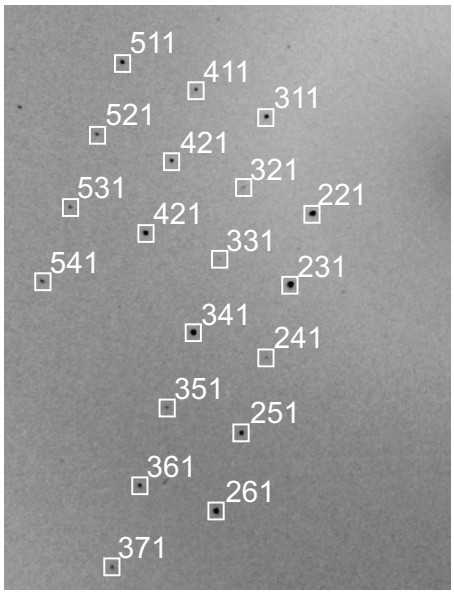

FIG. 3. A composite image from part of a data set (between $-2.5° \leq \omega \leq 2.5°$) collected at 9.5HPT, SRS from a methane A crystal at 9.1(2) GPa, with $a=8.508(7)$, $\alpha=89.32(3)$ Å. ω is the angle around the rotation axis.

III. ANALYSIS AND RESULTS

The first x-ray single-crystal data set (collected at ESRF) indexed to a rhombohedral unit cell consistent with the work of Nakahata *et al.*[14] with $a=8.269(7)$ Å and $\alpha=89.51(4)°$ at 13.6(2) GPa. The second data set (collected at SRS) indexed to a rhombohedral unit cell with lattice parameters of $a=8.508(7)$ Å and $\alpha=89.32(3)°$ at 9.1(2) GPa.

Observed reflection intensities were found to show clear violations of the symmetry conditions for the $\bar{3}m$ Laue group ($I(hkl)=I(lhk)=I(klh)=I(khl)=I(hlk)=I(lkh)$), but accord fully with the conditions of the $\bar{3}$ Laue group ($I(hkl)=I(lhk)=I(klh)\neq I(khl)=I(hlk)=I(lkh)$). This can be seen, for example, in the relative intensities $I(\sigma I)$ of 594(184), 680(131), 2115(268), and 2259(268) obtained for reflections (621), (162), (261), and (612), respectively, in the ESRF data set, which are the permutations (hkl), (lhk), (khl), and (hlk) of the Miller indices. This very clear discrimination is shown for these data overall by $R_{\text{merge}}(F^2)$ values of 0.35 and 0.30 in the $\bar{3}m$ Laue class for the first and second data sets, respec-

tively, and 0.06 and 0.05 (as already noted) in the $\bar{3}$ Laue class. Hence, the space group of methane A must be either $R\bar{3}$ or $R3$.

The positions of the carbon atoms were determined with the direct methods program SHELXS (Ref. 28) within the WINGX application.[29] This was done for each data set in each of the $R3$ and $R\bar{3}$ space groups. The (different) structures obtained in each space group both had 21 molecules in the unit cell and were the same for each data set. A unit cell containing 21 molecules is consistent with the equation of state of methane I and the pressure variation of the lattice parameters of methane A determined by Umemoto *et al.*,[7] given the requirement that methane A must be at least as dense as methane I at the same pressure.[10] For 21 molecules in a unit cell with the equation of state given by Nakahata *et al.*,[14] the density of methane A is ~2% greater than that of methane I. (20 molecules would thus be ~3% *less* dense than methane I.) The $R3$ solution had carbon atoms on three different onefold (x,x,x) sites and 18 carbon atoms on six threefold (x,y,z) sites. The $R\bar{3}$ solution had one carbon atom on a onefold site (0,0,0), two carbon atoms on a single twofold site (x,x,x), and 18 carbon atoms on three sixfold sites (x,y,z). Inspection of the $R3$ solution revealed that the six threefold carbon positions were close to being related in three pairs by a pseudoinversion center at one of the (x,x,x) sites, as also were the positions of the other two onefold (x,x,x) sites. It thus appeared that the two solutions were related by the presence of this pseudoinversion center in the $R3$ solution. Both solutions were then tested by structure refinement using GSAS.[27]

Refinement of the carbon positions and isotropic atomic displacement parameters (ADPs) with the second data set gave weighted R-factors $R_w(F^2)$ on F^2 and $R_w(F)$ on F of 11.7% and 5.7%, respectively, for $R3$ (30 parameters including a scale factor), and 13.8% and 6.7%, respectively, for $R\bar{3}$ (16 parameters including a scale factor). [Weighted R-factors based on structure-factors (F) are given here and in a similar context below as they are needed for the Hamilton significance test.[30] Otherwise R-factors based on squared structure-factors (F^2) or reflection intensities are used. These are normally approximately twice the magnitude of the R-factors based on F.] Based on the 124 reflections with F^2 greater than $3\sigma(F^2)$, this favors $R3$ with a confidence limit of 99.5% using the Hamilton significance test.[30] However, this preference for the $R3$ space group has to be treated with some caution as the hydrogen atoms have yet to be included in the description of the structure, and both the $R3$ and $R\bar{3}$ models were next tested against the neutron powder diffraction data.

For this, an initial model for the hydrogen positions is needed. The only available low-temperature diffraction data show that methane A does not undergo a detectable transition on cooling down to 10 K (Ref. 15) and so it seems reasonable to assume that the molecular orientations in methane A are ordered. (The validity of this assumption will be discussed later.) Molecular orientations that are fully ordered (in $R3$) or minimally disordered (in $R\bar{3}$) generate two possible distinct arrangements for each space group.

In $R3$, the three molecules centered on the threefold axis (x,x,x) sites can be orientationally ordered only if one of the H sites of each molecule is located on the threefold axis. There are two possible configurations for this: in one, the C–H bonds lying along the threefold axis are directed the same way for all three molecules (referred to as the +++ model), and in the other case one of these C–H bonds is oppositely directed to the other two (the ++− model). The remaining 18 molecules are all ordered and generated by six inequivalent molecules each centered on an x,y,z site in general orientations with four inequivalent H sites. (It is D sites and C–D bonds for the neutron diffraction case, but we will make the distinction only in presenting the neutron diffraction analysis.)

In $R\bar{3}$, the molecule on the inversion center at (0,0,0) must be disordered over at least two orientations—one with its C–H bond along the threefold axis in a positive direction and the other with the C–H bond in a negative direction. The orientations of the remaining methane molecules with carbon atoms on the threefold axis are related by the inversion center and for these molecules to be ordered they must have one H site on the threefold axis. There are then two possible configurations for these molecules: in one, both C–H bonds that are directed along the threefold axis have the H atom nearer the central molecule at (0,0,0) (the "in" model), and in the other these bonds have the H atom further from the central molecule (the "out" model). The remaining 18 molecules are all ordered and generated by three inequivalent molecules each centered on an x,y,z site in general orientations each with four inequivalent H sites.

Refinements of the neutron powder data were undertaken in GSAS (Ref. 27) using each of these four models. A rigid-body description of the methane molecule was used in which the D–C–D angles were fixed to have the values of an ideal tetrahedron. The initial value for all C–D bond lengths was set at 1 Å—close to the expected value of 1.042(5) Å found by Neumann *et al.*[9] for methane phase III. The positions of the centers of all the methane molecules and the molecular orientations were allowed to vary in each model according to the restrictions imposed by the site symmetry. For the molecules centered on general positions, all three Euler angles describing the molecular orientations were allowed to vary. For the molecules centered on the threefold axis, the need to keep one D site on the axis to maintain an ordered (or minimally disordered) molecule meant that only one Euler angle could be varied, corresponding to a rotation of the molecule about the C–D bond directed along the threefold axis. In addition to these parameters, a single C–D bond length, two isotropic ADPs (one for the carbon atoms and one for the deuterium atoms), and powder peak shape and background parameters were also varied. This gave an overall number of parameters of 59 for the $R3$ models and 40 for the $R\bar{3}$ models. The C–D bond length refined to values between 1.021(4) and 1.065(4) Å, depending on the model used, but all in good agreement with the expected value (above).

The weighted profile R-factors (R_{wp}, based on the quality of fit to the reflection intensities) obtained were 7.00% for the (+++) model (displayed in Fig. 4) and 7.06% for the

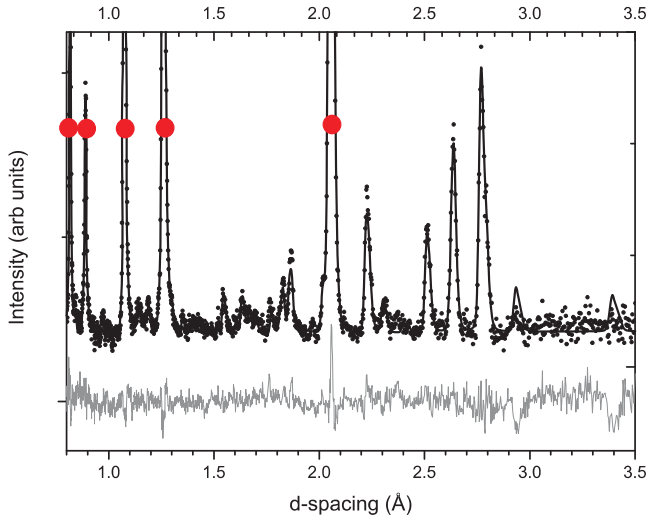

FIG. 4. A fit of the methane A structure to neutron powder-diffraction data using rigid-body tetrahedral methane molecules in the (+++) model in space group $R3$, as described in the text. The data were collected at 11.4(2) GPa and 110 K. The difference (gray line) between the observed (black dots) and fitted (black line) profiles is shown below the fit, and the red circles mark diamond reflections from the pressure-cell anvils. The refined lattice parameters were $a=8.326(1)$ Å and $\alpha=89.57(1)°$.

(++−) model in $R3$, as against 8.73% for the "in" and 8.36% for the "out" model in $R\bar{3}$. Use of statistical tests for powder data is difficult because the number of observations is not well defined, but in this case it is clear that the $R\bar{3}$ space group is again disfavored. The apparent marginal preference for the (+++) model over the (++−) model is not statistically significant given the small difference in R_{wp}, plus the fact that the sample was textured, and the relatively large number of parameters for a powder refinement. For the same reasons, and because of the differences in pressure and temperature between the x-ray and neutron studies, it is not possible to draw meaningful conclusions about the effects of deuteration on the structure of methane A from these data.

To obtain better evidence as to which model is correct, all four models were refined against the single-crystal x-ray data using GSAS.[27] Because the R_{merge} statistics are better for the second data set, collected at SRS at 9.1(2) GPa, results with these data will be given here, but the data set collected at ESRF yields the same conclusions. The rigid-body models used to refine the neutron data were adopted for these x-ray refinements, with the initial molecular orientations taken from those determined from the neutron refinements. The only difference from the neutron refinements was that the carbon atoms were no longer constrained to all have the same ADPs. A consequence of this is a larger difference in the number of parameters between the $R3$ and $R\bar{3}$ models than for the neutron refinements, because the $R3$ model has nine inequivalent carbon atoms and the $R\bar{3}$ model only five. There is then an overall number of parameters of 53 for the $R3$ models and 29 for the $R\bar{3}$ models including a scale factor.

The $R\bar{3}$ models gave $R_w(F^2)$ and $R_w(F)$ values of 10.1% and 4.9%, respectively, for the "in" model, and 10.7% and 5.1%, respectively, for the "out" model. For the $R3$ models, the $R_w(F^2)$ and $R_w(F)$ values were 8.3% and 4.0% for the (+++) model, and 8.7% and 4.2% for the (++−) model. From these R-factors, the $R\bar{3}$ models can be rejected with a confidence level of 97% using the Hamilton significance test.[30] This is slightly below the level of rejection for the carbon-only refinements above, but shows that a high level of preference for the $R3$ model remains with the hydrogens included. And for the $R3$ models, there is a preference for the (+++) model significant at the 99.5% level. The data cannot reject a small component of (++−) at the 10%–20% level, but we argue that the (+++) model is structurally more plausible and that any (++−) component is unlikely: the (++−) configuration requires that two of the molecules located on the threefold axis have C–H bonds directed toward each other (i.e., C−H···H−C), which is unlikely, whereas the (+++) model has these C–H bonds directed the same way (i.e., C−H···C−H). For all these reasons, we conclude that the space group of methane A is $R3$ and that the (+++) model is the correct molecular arrangement, with the refined atomic coordinates and ADPs given in Table I.

Finally, we return to the assumption made in solving the structure that the molecular orientations are fully ordered. As shown by the R-factors given above and by the values listed in Table I, the x-ray data are well able to determine the hydrogen atom positions and ADPs. First, the fits with ordered models give R-factors slightly better than those expected on the basis of the merging statistics, and Fourier difference maps calculated from these x-ray refinements show no evidence for systematic additional electron density not fitted by the ordered model. This strongly indicates that molecules are not disordered over two or more orientations. Second, the hydrogen atom ADPs in Table I are smaller than those found in methane III, the only ordered structure of methane previously known,[9] and this indicates that there is no significant disordering over more closely separated multiple sites. These results thus support the initial assumption of ordered molecular orientations made above on the basis that, although the $R3$ space group permits full ordering, no detectable change is observed in the methane A diffraction pattern on cooling down to 10 K.[15] A definitive experimental proof of full ordering would require high-resolution neutron diffraction data from a single-crystal sample, which is not currently feasible at pressures as high as 9–10 GPa.[16] But we conclude that any disordering is rather unlikely in view of the fits to the x-ray data.

IV. DISCUSSION

The structure of methane A has some similarities to CCP methane I in its molecular packing, but is overall quite strongly distorted from a CCP arrangement. The distortions away from close packing give rise to a much wider range of C–C distances than is found in methane I, with first-neighbor C–C distances ranging from 3.06 to 3.88 Å, whereas methane I would have a (single) first-neighbor C–C distance of 3.38 Å at the same density. (The choice of cutoff at 3.88 Å in methane A is somewhat arbitrary, but there is a gap in the C–C distance distribution between 3.88 and 4.12 Å.) Figure 5(a) shows the methane A structure in terms of the carbon

TABLE I. Carbon and hydrogen atom fractional coordinates and isotropic ADPs, U_{iso}, for the (+++) ordered model of the methane A structure at 9.1(2) GPa [spacegroup $R3$, a=8.508(7) Å and α=89.32(2)°], refined from single-crystal x-ray data as discussed in the text. H11 and H12 denote H atoms 1 and 2 of the C1 molecule, etc. The second column specifies the Wyckoff positions in the space group. The ADPs of the hydrogen atoms were constrained to be all the same, and refined to a value of 0.065(17) Å^2, as shown for atom H11. The refined C–H distance is 0.94(4) Å. As expected, this distance determined by x-ray diffraction is a little shorter than the internuclear C–D distance obtained from neutron diffraction data. A crystallographic information file of the methane A structure can be found in the supplementary material (Ref. 32).

Atom	Wyckoff position	x	y	z	U_{iso} (Å^2)
C1	1*a*	0.575(4)	0.575(4)	0.575(4)	0.042(7)
H11	1*a*	0.513(7)	0.513(7)	0.512(7)	0.065(17)
H12	3*b*	0.528(13)	0.588(21)	0.674(9)	0.065(-)
C2	1*a*	0.953(6)	0.954(6)	0.953(6)	0.05(2)
H21	1*a*	0.891(8)	0.891(8)	0.891(8)	0.065(-)
H22	3*b*	0.915(14)	1.057(7)	0.953(19)	0.065(-)
C3	1*a*	0.186(6)	0.187(7)	0.186(6)	0.07(3)
H31	1*a*	0.124(8)	0.124(8)	0.123(8)	0.065(-)
H32	3*b*	0.251(16)	0.249(17)	0.122(3)	0.065(-)
C4	3*b*	0.833(5)	0.291(4)	0.701(4)	0.074(14)
H41	3*b*	0.905(12)	0.214(10)	0.735(13)	0.065(-)
H42	3*b*	0.737(9)	0.245(13)	0.679(13)	0.065(-)
H43	3*b*	0.820(12)	0.366(12)	0.779(10)	0.065(-)
H44	3*b*	0.873(13)	0.339(14)	0.609(9)	0.065(-)
C5	3*b*	0.445(3)	0.318(4)	0.839(3)	0.006(5)
H51	3*b*	0.530(9)	0.373(13)	0.880(12)	0.065(-)
H52	3*b*	0.419(13)	0.236(10)	0.906(11)	0.065(-)
H53	3*b*	0.359(9)	0.387(10)	0.828(13)	0.065(-)
H54	3*b*	0.473(13)	0.279(13)	0.740(7)	0.065(-)
C6	3*b*	0.720(4)	0.626(4)	0.953(4)	0.024(8)
H61	3*b*	0.724(12)	0.707(11)	1.026(1)	0.065(-)
H62	3*b*	0.707(14)	0.530(8)	1.005(13)	0.065(-)
H63	3*b*	0.636(10)	0.644(13)	0.885(11)	0.065(-)
H64	3*b*	0.814(9)	0.624(13)	0.895(12)	0.065(-)
C7	3*b*	0.519(4)	0.189(4)	0.435(5)	0.047(12)
H71	3*b*	0.448(11)	0.261(11)	0.392(13)	0.065(-)
H72	3*b*	0.486(13)	0.161(13)	0.536(7)	0.065(-)
H73	3*b*	0.524(13)	0.100(9)	0.372(11)	0.065(-)
H74	3*b*	0.619(8)	0.235(12)	0.440(12)	0.065(-)
C8	3*b*	0.938(4)	0.072(4)	0.420(4)	0.033(9)
H81	3*b*	0.983(12)	0.172(8)	0.416(15)	0.065(-)
H82	3*b*	0.951(15)	0.031(14)	0.524(8)	0.065(-)
H83	3*b*	0.832(7)	0.079(12)	0.399(14)	0.065(-)
H84	3*b*	0.989(11)	0.006(13)	0.350(12)	0.065(-)
C9	3*b*	0.204(4)	0.085(4)	0.703(4)	0.039(9)
H91	3*b*	0.253(14)	0.039(13)	0.790(11)	0.065(-)
H92	3*b*	0.171(12)	0.187(9)	0.728(14)	0.065(-)
H93	3*b*	0.276(11)	0.090(14)	0.619(10)	0.065(-)
H94	3*b*	0.118(9)	0.025(12)	0.674(13)	0.065(-)

positions of 33 carbon atoms (about 1.5 unit cells), linked by lines showing nearest-neighbor contacts to define layerlike units that can be compared with the A, B, and C layers of CCP. As can be seen from the outline of the rhombohedral unit cell, the layer units are viewed along a direction nearly perpendicular to the threefold axis, which is the ⟨111⟩ direction of the unit cell. The "layers" are meaningful over the range shown in Fig. 5(a), but, as discussed below (and illustrated in Fig. 6), they are not parts of extended discrete layers, unlike in CCP. They are layerlike structural units on the length scale of a unit cell, and "layer" is used with this meaning in discussing the methane A structure. As specified in the caption to Fig. 5, the layerlike units 1–5 are labeled L1 to L5 with a letter, A′, B′ (or B″), and C′, added according to their closest correspondence to the (true) A, B, and C layers of the CCP structure, which is shown from the same viewing perspective in Fig. 5(e). (B″ and B′ are distorted in different ways from the B layer of CCP.) It can be seen immediately that the methane A layers are quite significantly puckered in Fig. 5(a), and that the local stacking sequence in methane A most closely resembles an ABCBB sequence instead of the ABCABC of the CCP structure.

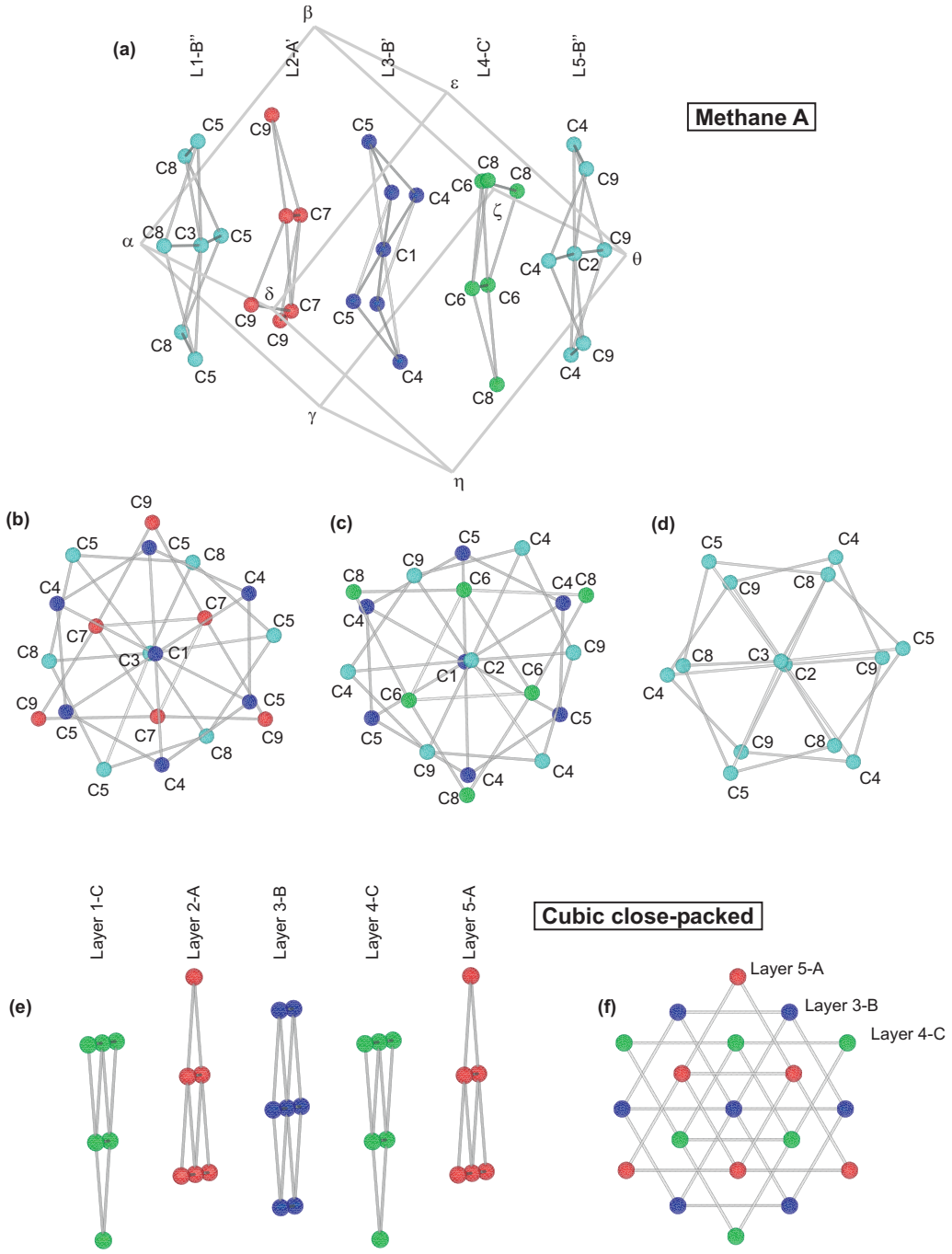

FIG. 5. The arrangement of the carbon atoms in phase A and a comparison with the arrangement of the CCP structure of methane I. (a) shows the carbon-atom structure in terms of five pseudo-close-packed, puckered layer units, numbered L1 to L5, viewed approximately perpendicularly to the ⟨111⟩ direction (the threefold axis). The rhombohedral unit cell is shown in outline, with vertices lettered from α to θ as referred to in the text. The layer units do not extend as true layers through the structure (see the text for discussion of Fig. 6), but can be defined on this scale for comparison with the true extended (unpuckered) layers of the CCP structure. (b)–(d) show views approximately along the ⟨111⟩ direction, viewing in the direction from θ toward α, for selected layer units. (e) and (f) show corresponding views of the CCP structure, which is a stacking of close-packed layers in three different positions, A (red), B (dark blue), and C (green). In (a), the layer units are identified according to closeness of correspondence to A, B, and C, and accordingly labeled L1-B″, L2-A′, etc., where "L" denotes "layer unit" in each case. B′ and B″ are both closest to B in that they have a central atom in the B position, but differ in the way they are distorted from B: the B″ layer units are shown light blue to distinguish them from the B′ ones (see text). The views along ⟨111⟩ for methane A (in the direction from θ toward α) show (b) L1-B″, L2-A′, and L3-B′; (c) L3-B′, L4-C′, and L5-B″; and (d) L5-B″ in one unit cell below L1-B″ in the next. The carbon atoms are labeled C1, C2, etc. as in Table I.

Figure 5 shows a view approximately along the threefold axis (b) for L1-B″, L2-A′, and L3-B′, (c) for L3-B′, L4-C′, and L5-B″, and (d) for L5-B″ plus L1-B″ in the next unit cell. The BB-like sequence in (d) is a particularly marked departure from close packing. The corresponding view of CCP is shown in Fig. 5(f). It can be seen in Figs. 5(b)–5(d) how L1-B″, L3-B′, and L5-B″ have at their centers the C3, C1, and C2 atoms that lie on (x,x,x) sites along the threefold axis. It can also be seen in (a), (b), and (c) that L3-B′ (in dark blue) is close to being a centrosymmetric arrangement

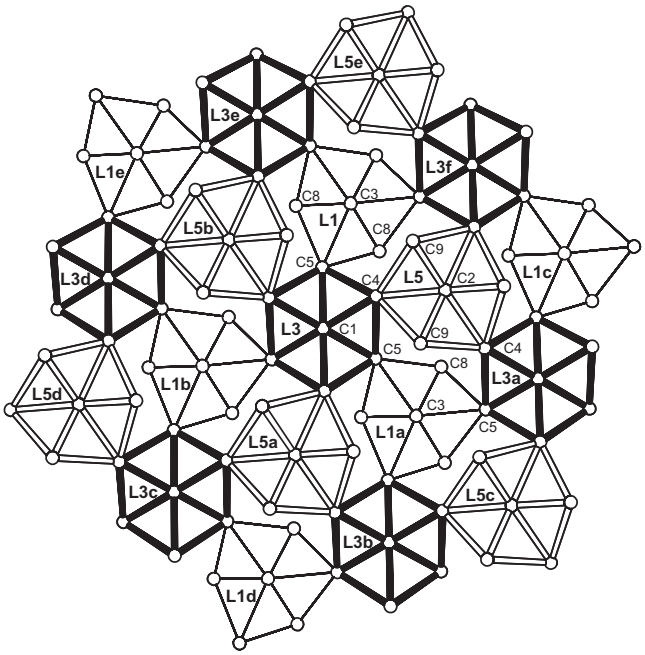

FIG. 6. The carbon arrangement of methane A viewed along the threefold axis (in the direction from θ toward α) showing the arrangement around an L3-B′ layer unit of Fig. 5(a), here labeled simply L3. The first ring around L3 is made up of L1-B″ units labeled L1, L1a, and L1b, and L5-B″ units labeled L5, L5a, and L5b. The second ring is made up of L3 units, L3a to L3f; L1 units, L1c to L1e; and L5 units, L5c to L5e. Each of the groups of units L1, L3, and L5 is distinguished by the way its nearest-neighbor contacts are shown—by thin, thick, and double lines, respectively. The L3 units are all in a common plane perpendicular to the threefold axis; and the L1 and L5 units are in planes, respectively, $X/3$ below and $X/3$ above the L3 plane, where X is the average separation along the threefold axis of the layer units in Fig. 5(a). Some of the carbon atoms are labeled as in Fig. 5.

about its central C1 atom. This is a pseudocenter that would be a true center of symmetry in the $R\bar{3}$ structure, as discussed in Sec. III. This pseudocenter at the C1 site also relates L2-A′ (in red) to L4-C′ (in green), and L1-B″ to L5-B″ (both light blue). The other pseudocenter is thus between C2 and C3 in Fig. 5(d), where it can be seen that L5-B″ is close to being an inversion of L1-B″ through that point. Figure 5(a) shows that all five layer units are puckered to a similar extent. But in (b), (c), and (d) it can be seen that L2-A′, L3-B′, and L4-C′ are close to a regular close-packed (two-dimensional hexagonal) arrangement in projection along the threefold axis, whereas L1-B″ and L5-B″ are both quite strongly distorted. Nonetheless, the sequence of L2-A′, L3-B′, and L4-C′ is still quite far from CCP because L3-B′ is rotated 30° around the threefold axis from the orientation that layer B has with respect to the A and C layers in CCP [Fig. 5(f)].

Figure 6 shows how the layer units of Fig. 5(a) extend into the full three-dimensional structure. At the center is L3-B′ of Fig. 5(a), here labeled simply L3, with its central C1 atom also labeled. If the representative five-layer part of the structure shown in Fig. 5(a) is associated with the lattice point (unit-cell vertex) labeled α, then there must be the same five-layer arrangements similarly associated with the lattice points labeled β, γ, and δ. These are 120° apart around the threefold axis (through lattice point α), and displaced along the threefold axis direction by 1/3 of the repeat distance from α to θ. This displacement is $5X/3$ where X is the average separation of the layer units in Fig. 5(a). Thus, L1-B″ of Fig. 5(a) appears in three positions 120° apart around L3 in Fig. 6, as labeled L1, L1a, and L1b. But their centers lie in a common plane that is $X/3$ *below* the plane of L3 (which is $6X/3$ from the center of L1-B″). These L1 units are linked to the L3 unit via shared C5 atoms as shown, which is made possible by the puckering of the units: it can be seen in Fig. 5(a) that the puckering of L3-B′ places the shared C5 atoms to the left of the central C1 as viewed, which locates them, as said, below the C1 of L3 in Fig. 6. In a similar way, lattice points ϵ, ζ, and η bring L5-B″ of Fig. 5(a) to the positions labeled L5, L5a, and L5b in Fig. 6, and their centers lie in a common plane $X/3$ *above* L3. The L3 and L5 units share C4 atoms as shown, and these can be seen to lie to the right of the central C1 in the L3-B′ unit of Fig. 5(a), and thus above C1 of L3 in Fig. 6. Both L1 and L5 are B-like layer units, and each has a threefold axis through its central atom. Applying the threefold symmetry of the axes through these L1 and L5 layer units generates the further L1, L3, and L5 units shown in the outer ring of Fig. 6.

The overall sequence of layer units along a given threefold axis, over the repeat distance from α to θ, is L4, L1, L3, L5, L2, L4, L1, L3, L5, L2, L4, L1, L3, L5, L2, L4, L1, L3, L5, and L2, with centers all $X/3$ apart. The arrangement in Fig. 6 is made up of the L1, L3, and L5 units at the center of this sequence, and shows how a consecutive sequence of three units is needed to give approximate close-packed space filling in projection onto the plane perpendicular to the threefold axis. Immediately above this—that is, nearer to θ—is a similar three-unit arrangement in which the L1, L3, and L5 of Fig. 6 are replaced by, respectively, L2, L4, and L1, to make an arrangement in which the L2 lie below L4, and the L1 lie above L4. The L5 units of Fig. 6 thus have adjacent L2 units with centers $X/3$ above the centers of the L5 units, and these share the C9 atoms shown as unshared in Fig. 6. Likewise, the C8 atoms of L1 shown as unshared in Fig. 6 are shared with the L4 units of the three-unit arrangement (of L5, L2, and L4) that lies below the arrangement in Fig. 6.

In this way, the structure can be regarded as comprising five three-unit arrangements along the threefold axis direction: L4/L1/L3, L5/L2/L4, L1/L3/L5, L2/L4/L1, and L3/L5/L2. This is arbitrary to the extent that—as explained—*all* units share atoms with adjacent units above and below them. And there is no meaning to separating this continuous arrangement into three-unit groups other than that this gives approximate space filling in projection onto a plane perpendicular to the threefold axis, and provides a way of showing how the structure is related to CCP. It can be seen in Fig. 6 that the arrangement of the L1, L3, and L5 units is far from a true close-packed layer in projection, but close packing can be recovered as follows.

Consider the region between L3 and L3a in Fig. 6. The C8 and C9 atoms are—as explained above—shared with units in the three-unit arrangements above and below the one in Fig. 6. In order to separate the three-unit arrangements from one another—as required to recover close-packed separate layers—these atoms can be regarded as 50% in L1/L3/L5, and 50% in L5/L2/L4 or L2/L4/L1. If all the units in the

L1/L3/L5 arrangement of Fig. 6 are then rotated a little to allow the C8 and C9 "half" atoms to coalesce, it can be seen that they become the single (100%) central atom of a hexagon made up of C4, C2, C4, C5, C3, and C5. (Of course, this also requires that all the puckering and the $X/3$ steps between L1, L3, and L5 are reduced to zero, so all atoms in the L1/L3/L5 arrangement are brought into a common plane.) Given also small displacements so that all the hexagons become similar and regular, a close-packed arrangement in the layer is recovered. There would then be five such separated, close-packed layers, but still stacked ABCBB, and relative displacements in the plane of the layers would be needed finally to recover a CCP structure.

The rotations of the units, and removal of the puckering, needed to recover a close-packed layer would slightly decrease the density of molecules in the layer compared with that in the projection of the L1/L3/L5 arrangement. But this reduced density in the close-packed layers is counterbalanced by a smaller layer spacing in CCP: the average spacing of the layer units in Fig. 5(a) is 2.97 Å, whereas the layer spacing in a CCP structure of the same density would be 2.76 Å. The larger spacing in methane A is attributable to puckering of the layer units—giving them greater extent along the threefold axis direction—and the non-close-packed ABCBB-like stacking.

In summary, there are localized regions in the structure of methane A that have similarities to a CCP arrangement, but everywhere the structure is significantly distorted from CCP, in a number of different ways and to varying degrees. The arrangement of the molecular orientations seems to suggest that these are largely determined by steric effects. In the structure there are no orientations where two C–H bonds are directed toward each other [for the final (+++) configuration, as discussed above] and very few where a C–H bond is directed toward another carbon atom. Instead, the common arrangement is with molecules oriented so as to maximize the H···H distances. Thus, the distortion of the structure of methane A away from close packing can be regarded as the result of the competition between the need to avoid close H···H contacts and the tendency of spherical or quasispherical objects to adopt close packing as the densest arrangement. Hence, it appears reasonable to suggest that the transition from methane I is driven by the increasing influence of the molecular anisotropy on the crystal structure by the application of pressure.

Nakahata *et al.*[14] pointed out the similarity of the unit cell and powder patterns of methane A to those of a phase found in CF_4 and CCl_4 at low temperature or under moderate pressure at room temperature. Phase I of CF_4 forms at ambient pressure on cooling below 89.5 K (Ref. 31) and on application of pressure to 1.86 GPa at room temperature.[33] This phase has been indexed on a rhombohedral unit cell with $a=11.577(9)$ Å and $\alpha=89.49(1)°$.[34] Phase Ib of CCl_4 forms from the liquid at room temperature and a pressure of 0.13 GPa, or on cooling below ~240 K at ambient pressure.[35] It has been indexed on a rhombohedral unit cell with $a=14.24$ Å and $\alpha=90°$.[36] Several different authors have concluded that both CCl_4 Ib and CF_4 I contain 21 molecules in their unit cells, and have noted the similarities of their powder diffraction patterns.[34,36,37] The similarity of the symmetry, dimensions, and contents of the unit cells of CF_4 phase I, CCl_4 phase Ib, and methane phase A, combined with the similarities between CH_4, CF_4, and CCl_4 as nonpolar tetrahedral molecules, suggests that all these phases may adopt the same structure. It would clearly be of considerable interest to verify this by solving the as yet unknown structures of the rhombohedral phases of CF_4 and CCl_4. This is particularly of interest because, if the distorted close-packed structure determined here for methane A is indeed also that of CF_4 and CCl_4, this would add a new structure to the seven packing types so far identified for EX_4 compounds.[38]

If methane, CF_4 and CCl_4 do prove to share this rhombohedral structure, it would also be of interest to understand why it is the only known structure that is common to all three. CF_4 and CCl_4 transform under pressure to monoclinic structures ($P2_1/c$) with four molecules in the unit cell.[20,39] Methane does not subsequently transform to a monoclinic structure with pressure, but instead transforms to a structure with a large cubic unit cell.[40] It should be noted that the Pauling electronegativity decreases from fluorine to chlorine to hydrogen and it may be that the degree to which the C–X (X being H, Cl, or F) bonds are polarized is the cause of the differing structural sequence.

V. CONCLUSIONS

We have determined the crystal structure of phase A of methane, a high-pressure phase which forms at 5.2 GPa at room temperature. The crystal structure was determined from a series of *in situ* diffraction studies using both x-ray and neutron techniques. X-ray single-crystal diffraction results enabled us to solve the molecular packing arrangement, which was used as a basis for the determination of the hydrogen (deuterium) positions from neutron powder diffraction data. The hydrogen positions were then used for further refinement of the structure against x-ray data, which enabled us to resolve and discuss additional subtleties in the molecular arrangements and to justify the assignment of the structure to the $R3$ space group with 21 molecules in the unit cell. The structure is quite strongly distorted from a CCP arrangement and we present evidence that it has ordered molecular orientations. This is consistent with orientational order being produced by the increasing effects of anisotropy in the intermolecular interactions as the density is increased. Furthermore, similarities to the unit cell contents and symmetry for CF_4 and CCl_4 lead us to suggest that this structure may be common to the carbon tetrahalides.

Our results also provide crucial experimental data for testing computational models of methane under planetary conditions. The solution of the structure of phase A extends the pressure range over which the density of methane is definitively known to beyond 10 GPa and places extrapolations of the equation of state at pressures beyond this on a firmer footing. Density is an important parameter in calculations of methane under planetary conditions,[41] and this extension of the equation of state provides a new benchmark for that. Furthermore, knowledge of the full structure of methane in the 10 GPa region provides a starting point for new modeling

of higher-pressure solid phases, in the way that the solution of ammonia IV structure[42] was used as a basis for calculations of the states in ammonia in the megabar (100 GPa) range.[3]

ACKNOWLEDGMENTS

We would like to thank A. Lennie and M. Hanfland for support and assistance in using, respectively, stations 9.5HPT (SRS) and ID09a (ESRF), L. F. Lundegaard for advice and help with the treatment and reduction of the x-ray data, and D. J. Francis for technical assistance with the neutron experiment on the HiPR/PEARL instrument (ISIS). The x-ray diffraction experiments at ESRF were performed as part of Long Term Project HS3090 on single-crystal diffraction at extreme conditions. This work was funded by the U.K. Engineering and Physical Science Research Council and supported by the U.K. Science and Technology Facilities Council through access to beamtime and other resources.

[1] T. Guillot, Annu. Rev. Earth Planet Sci. **33**, 493 (2005).
[2] S. Stanley and J. Bloxham, Nature (London) **428**, 151 (2004).
[3] C. Cavazzoni, G. L. Chiarotti, S. Scandolo, E. Tosatti, M. Bernasconi, and M. Parrinello, Science **283**, 44 (1999).
[4] J. F. Lin, E. Gregoryanz, V. V. Struzhkin, M. Somayazulu, H. K. Mao, and R. J. Hemley, Geophys. Res. Lett. **32**, L11306 (2005).
[5] S. Ninet and F. Datchi, J. Chem. Phys. **128**, 154508 (2008).
[6] R. Bini and G. Pratesi, Phys. Rev. B **55**, 14800 (1997).
[7] S. Umemoto, T. Yoshii, Y. Akahama, and H. Kawamura, J. Phys.: Condens. Matter **14**, 10675 (2002).
[8] W. Press, J. Chem. Phys. **56**, 2597 (1972).
[9] M. A. Neumann, W. Press, C. Nöldeke, B. Asmussen, M. Prager, and R. M. Ibberson, J. Chem. Phys. **119**, 1586 (2003).
[10] R. M. Hazen, H. K. Mao, L. W. Finger, and P. M. Bell, Appl. Phys. Lett. **37**, 288 (1980).
[11] P. Hebert, A. Polian, P. Loubeyre, and R. LeToullec, Phys. Rev. B **36**, 9196 (1987).
[12] M. M. Thiéry, D. Fabre, and K. Kobashi, J. Chem. Phys. **83**, 6165 (1985).
[13] R. Bini, L. Ulivi, H. J. Jodl, and P. R. Salvi, J. Chem. Phys. **193**, 1354 (1995).
[14] I. Nakahata, N. Matsui, Y. Akahama, and H. Kawamura, Chem. Phys. Lett. **302**, 359 (1999).
[15] H. E. Maynard, J. S. Loveday, S. Klotz, C. L. Bull, and T. C. Hansen, High Press. Res. **29**, 125 (2009).
[16] C. L. Bull, M. Guthrie, R. J. Nelmes, J. S. Loveday, H. Hamidov, and M. J. Gutmann, High Press. Res. **29**, 644 (2009).
[17] J. M. Besson, R. J. Nelmes, G. Hamel, J. S. Loveday, G. Weill, and S. Hull, Physica B **180–181**, 907 (1992).
[18] L. Merrill and W. A. Bassett, Rev. Sci. Instrum. **45**, 290 (1974).
[19] R. Boehler and K. De Hantsetters, High Press. Res. **24**, 391 (2004).
[20] G. J. Piermarini and A. B. Braun, J. Chem. Phys. **58**, 1974 (1973).
[21] H. K. Mao, J. Xu, and P. M. Bell, J. Geophys. Res. **91**, 4673 (1986).
[22] L. F. Lundegaard, C. Guillaume, M. I. McMahon, E. Gregoryanz, and M. Merlini, J. Chem. Phys. **130**, 164516 (2009).
[23] Deuteration eliminates the high background given by incoherent neutron scattering from hydrogen atoms.
[24] W. G. Marshall and D. J. Francis, J. Appl. Crystallogr. **35**, 122 (2002).
[25] S. Klotz, M. Gauthier, J. M. Besson, G. Hamel, R. J. Nelmes, J. S. Loveday, R. M. Wilson, and W. G. Marshall, Appl. Phys. Lett. **67**, 1188 (1995).
[26] W. G. Marshall, Program ATTEN: An attenuation correction calculation for the Paris-Edinburgh cell on the PEARL/HiPr Diffractometer at ISIS, ISIS Facility, Rutherford Appleton Laboratory, Chilton, Didcot, Oxfordshire OX11 0QX, UK.
[27] A. C. Larson and R. B. Von Dreele, Los Alamos National Laboratory Technical Report No. LAUR 86-748, 1994.
[28] G. M. Sheldrick, Acta Crystallogr., Sect. A: Found. Crystallogr. **46**, 467 (1990).
[29] L. J. Farrugia, J. Appl. Crystallogr. **32**, 837 (1999).
[30] W. C. Hamilton, Acta Crystallogr. **18**, 502 (1965).
[31] S. C. Greer and L. Meyer, J. Chem. Phys. **51**, 4583 (1969).
[32] See supplementary material at http://dx.doi.10.1063/1.3455889 for a crystallographic information file for the methane A structure.
[33] S. Sasaki, Y. Ikeda, and H. Shimizu, J. Phys. Soc. Jpn. **60**, 1560 (1991).
[34] A. N. Fitch and J. K. Cockcroft, Z. Kristallogr. **203**, 29 (1993).
[35] K. Kotake, N. Nakamura, and H. Chihara, Bull. Chem. Soc. Jpn. **40**, 1018 (1967).
[36] C. E. Weir, G. J. Piermarini, and S. Block, J. Chem. Phys. **50**, 2089 (1969).
[37] R. Rudman and B. Post, Science **154**, 1009 (1966).
[38] A. K. Wolf, J. Glinnemann, and M. U. Schmidt, Cryst. Eng. Comm. **10**, 1364 (2008).
[39] D. Shindo, T. Yoshii, Y. Akahama, and H. Kawamura, J. Phys.: Condens. Matter **14**, 10653 (2002).
[40] H. E. Maynard-Casely, Ph.D. thesis, University of Edinburgh, 2009.
[41] F. Ancilotto, G. Chiarotti, S. Scandolo, and E. Tosatti, Science **275**, 1288 (1997).
[42] J. S. Loveday, R. J. Nelmes, W. G. Marshall, J. M. Besson, S. Klotz, and G. Hamel, Phys. Rev. Lett. **76**, 74 (1996).